Purdue University
Purdue e-Pubs

International Compressor Engineering Conference | School of Mechanical Engineering

2010

Study of the Endface Friction of the Revolving Vane Mechanism

Alison Subiantoro
School of Mechanical and Aerospace Engineering

Kim Tiow Ooi
School of Mechanical and Aerospace Engineering

Follow this and additional works at: http://docs.lib.purdue.edu/icec

Subiantoro, Alison and Ooi, Kim Tiow, "Study of the Endface Friction of the Revolving Vane Mechanism" (2010). *International Compressor Engineering Conference.* Paper 1945.
http://docs.lib.purdue.edu/icec/1945

This document has been made available through Purdue e-Pubs, a service of the Purdue University Libraries. Please contact epubs@purdue.edu for additional information.
Complete proceedings may be acquired in print and on CD-ROM directly from the Ray W. Herrick Laboratories at https://engineering.purdue.edu/Herrick/Events/orderlit.html

Study of the Endface Friction of the Revolving Vane Mechanism

Alison SUBIANTORO[1]*, Kim Tiow OOI[2]

Nanyang Technological University,
School of Mechanical & Aerospace Engineering,
Thermal & Fluids Engineering Division,
Singapore
[1]+65 6790 4674, alis0004@ntu.edu.sg,
[2]+65 6790 5511, mktooi@ntu.edu.sg

ABSTRACT

The Revolving Vane (RV) mechanism is different from other rotary machines because the rotor and the cylinder rotate together eccentrically. This produces a unique situation in the endface gaps. A theoretical study on the friction behavior in these gaps has been conducted. It is found that due to the eccentricity, a resultant force is produced by the endface friction. The power loss is also found to be not only affected by the velocity difference, but also by the eccentricity. A region in between the rotor and the cylinder axis is found to suffer from high friction loss due to high velocity difference occurring there. Comparisons with common rotary machines show that RV mechanisms produce smaller endface friction loss when the ratio between the rotor and the cylinder radii is less than 0.6.

1. INTRODUCTION

Rotary machines were originally developed to solve the problems faced by the more established reciprocating machines. They include the vibration and noise issues. In their further development, rotary machines have since gained increased popularity due to their compactness and good vibration characteristics. However, rotary machines usually have issues with mechanical efficiencies due to significant frictional losses caused by the high relative velocities among the sliding parts. For example, high relative speeds between sliding components such as the eccentric and the piston result in significant loss in rolling piston compressors (Yanagisawa and Shimizu, 1985).

The revolving vane (RV) mechanism was invented to solve these problems (Teh and Ooi, 2006). In this mechanism, the cylinder rotates together with the rotor at their respective axis of rotation, resulting in much reduced relative velocities between the moving components. Further studies have shown that the mechanism indeed has superior mechanical efficiencies as compared to the more established rotary machines (Teh and Ooi, 2009a). Experiments have also been conducted confirming that the design concept can operate successfully (Teh and Ooi, 2009b). The design concept has also been adopted for expanders (Subiantoro and Ooi, 2009, 2010).

There are two endfaces gaps in the RV mechanism as can be seen from Figure 1, irrespective of how the bearings are arranged. In each of these gaps, lubricant mixed with the working fluid move due to shear and pressure, causing friction on the endface walls. One of the frictions that have been reduced significantly by the RV mechanism is at these endface gaps (Teh and Ooi, 2009a). This is possible since the relative velocity between the rotor and the cylinder is now reduced, resulting in smaller endface friction loss. However due to the eccentric nature of the rotations of the two components, it is possible that this endface friction loss becomes significant when inappropriately designed. In addition, the fact that the cylinder and the rotor rotate together eccentrically in the RV mechanism produces an interesting situation at the endface gaps rarely encountered in typical rotary machines.

It is the purpose of this paper to investigate in more detail the friction behaviors at the endfaces of the rotating components of the RV mechanism. The study was conducted by analyzing the endface friction of the mechanism theoretically. A comparison with the endface friction of a typical rotary mechanism, such as the sliding vane

machine, where only the rotor is rotating while the cylinder is stationary, will also be conducted to observe how RV mechanism compares to a typical rotary machine.

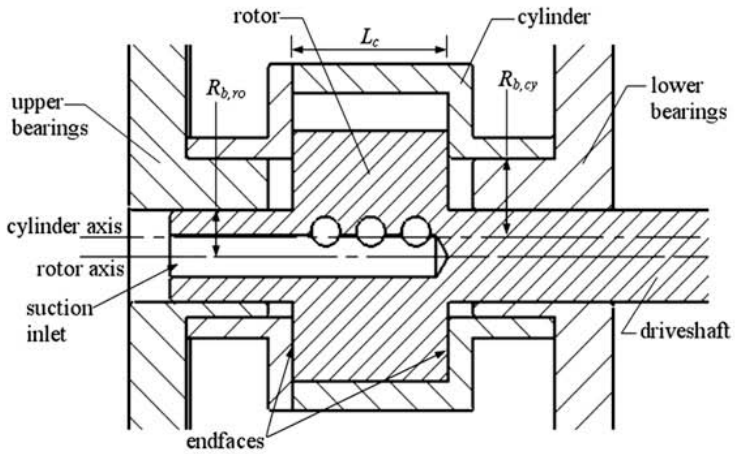

Figure 1: Side-view of the RV compressor (Teh and Ooi, 2009a)

2. THEORETICAL MODEL OF THE RV MECHANISM

The endface area occupied by the vane is relatively small and is neglected to simplify the analysis. Hence, the areas of interest can be either one of the two shapes shown as the shaded areas in Figure 2. The larger circle is the cylinder wall while the smaller one is the rotor wall. The "x" sign with a "C" next to it refers to the axis of the cylinder while the one with an "R" is the axis of the rotor. The small hole concentric to the cylinder in Figure 2(a) represents the cylinder shaft hole.

The area in Figure 2(a), which is of the shape of a circle with a hole that is eccentric from the center of the circle, is found at both the endfaces when the bearings are arranged in the simply-supported arrangement like Figure 1 or at the side with the rotor shaft when the bearings are arranged in the cantilever-type arrangement. The shape in Figure 2(b), which is a solid circle, is found only at the side without the rotor shaft when the bearings are arranged in the cantilever-type arrangement. It is also important to remember that the area of interest is actually applicable for both the rotor and cylinder endfaces and that there are two endface gaps in a RV machine.

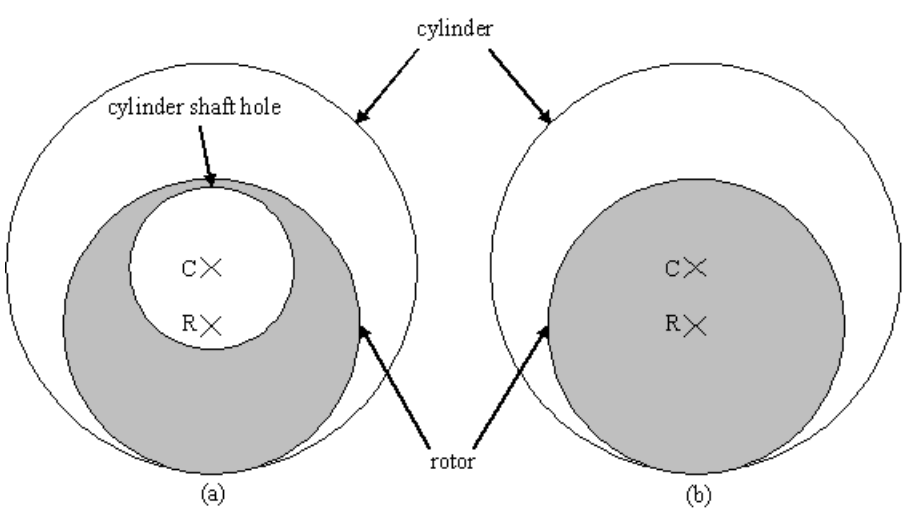

Figure 2: The two possible endface areas of interest

In this study, for simplicity, the area of interest is taken to be the one shown in Figure 2(b) only. The rotor is set to be the driving component and to rotate at a constant velocity in the clockwise direction, ω_r, while the cylinder is the driven component. It is assumed that the fluid in the endface gaps is a homogeneous lubricant with a constant viscosity, μ. The width of the endface gaps, δ, is assumed to be uniform and constant throughout the operation. It is also assumed that the gaps are narrow enough such that pressure effect to the fluid flow is insignificant. Instead, the fluid only flows due to shear according to the Couette flow model expressed by Equation (1). The velocity difference in Equation (1), ΔV, is the cylinder velocity vector minus the rotor velocity vector when dealing with the rotor endface and is the opposite when dealing with the cylinder endface. From Equation (1), the resultant force and torque loss produced by the fluid friction in the endface gaps can be derived and were found to be as expressed by Equations (2) and (3) respectively.

$$\vec{\tau} = \frac{\mu}{\delta}\Delta\vec{V} \tag{1}$$

$$\vec{F} = \frac{\mu}{\delta}\int \Delta\vec{V}dA \tag{2}$$

$$\vec{T} = \frac{\mu}{\delta}\int \left(\Delta\vec{V}\times\vec{r}\right)dA \tag{3}$$

It is important to note that the moment arm, r, in Equation (3) is referenced to the rotor axis when analyzing the rotor endface and is referenced to the cylinder axis when analyzing the cylinder endface.

2.1 Rotor Endface

The analysis is started at the rotor endface since the area of interest is concentric to the rotor endface. Taking an arbitrary point A in the area of interest, a triangle made of point A, the cylinder axis, C, and the rotor axis, R, can be drawn as shown in Figure 3.

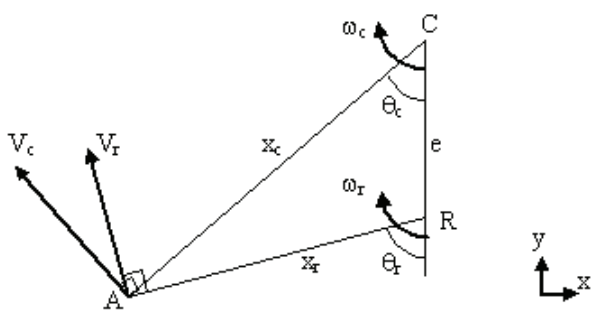

Figure 3: The ACR triangle

Applying cosine and sine rules to the ACR triangle, the velocity difference vector at point A can be expressed as in Equation (4).

$$\vec{V}_c - \vec{V}_r = \left(-\omega_c e - (\omega_c - \omega_r)x_r \cos\theta_r\right)\hat{x} + \left((\omega_c - \omega_r)x_r \sin\theta_r\right)\hat{y} \tag{4}$$

Observing Figure 3 and Equation (4), it can be seen that the maximum velocity difference occurs in the region between the rotor axis, R, and the cylinder axis, C. Here, the rotor velocity vector points to the positive x-direction while the cylinder velocity vector points to the negative x-direction. The maximum endface friction loss will therefore be large in this region. In light of this finding, it is advantageous to remove the friction from this region. This is the case when our area of interest is the one shown in Figure 2(a).

Substituting Equation (4) into Equations (2) and (3) gives the resultant force and the torque produced by the endface friction at the rotor endface which are expressed by Equations (5) and (6) respectively.

$$\vec{F}_r = \left(-\frac{\mu}{\delta} \pi \omega_c e r_r^{\,2} \right) \hat{x} + 0\,\hat{y} \tag{5}$$

$$\vec{T}_r = \left(\frac{\mu}{\delta} \frac{\pi}{2} (\omega_c - \omega_r) r_r^{\,4} \right) \hat{z} \tag{6}$$

It is interesting to observe that the resultant force acting on the rotor endface does not have a y-component. It is simply a force vector that always points to the negative x-direction. The magnitude is also interestingly proportional to the area of the rotor endface multiplied by the tangential velocity of the cylinder acting at the rotor axis. It is not a function of the velocity difference at all. To give some illustration on how strong this force is, an 18 mm rotor radius and 25 mm radius RV machine with the rotor turning at a constant angular velocity of 3000 rpm is used. The endface gap is 7.5μm and the lubricant viscosity is 0.0034 Pa.s. With this configuration, the average resultant force is found to be around 1.0 N only.

As for the torque, the value can be either positive or negative depending on the difference between the cylinder and rotor angular velocities. When the cylinder angular velocity is higher than the rotor, it is as if the cylinder tries to pull the rotor to move faster through the fluid in the gaps thus producing a positive torque to the rotor. On the other hand, when the rotor is turning faster than the cylinder, it is as if the rotor is pulling the cylinder and hence a negative torque, indicating a torque loss at the rotor, is obtained.

2.2 Cylinder Endface

Performing a similar procedure described in section 2.1 to the cylinder endface gives the resultant force and torque as expressed by Equations (7) and (8) respectively.

$$\vec{F}_c = \left(\frac{\mu}{\delta} \pi \omega_c e r_r^{\,2} \right) \hat{x} + 0\,\hat{y} \tag{7}$$

$$\vec{T}_c = -\frac{\mu}{\delta} \left(\pi \omega_c e^2 r_r^{\,2} + \frac{\pi}{2} (\omega_c - \omega_r) r_r^{\,4} \right) \tag{8}$$

Equation (7) shows that the resultant force acting on the cylinder endface is just the opposite of the one acting at the rotor. This is expected since both the rotor and the cylinder never move laterally, only rotationally. Meanwhile, Equation (8) shows that the torque on the cylinder endface is equal to the negative of the torque acting on the rotor endface and a component which is the result of the eccentricity between the rotor and the cylinder axis. If the rotor and the cylinder axis are located at the same location, the eccentric component of Equation (8) disappears. This eccentric component is also equal to the magnitude of the resultant force multiplied with the eccentricity, e.

2.3 RV Mechanism

Combining Equations (6) and (8) together with their respective angular velocities gives the total power loss of the RV mechanism caused by the endface friction expressed by Equation (9).

$$P = -\frac{\mu}{\delta} \left(\pi \omega_c^{\,2} e^2 r_r^{\,2} + \frac{\pi}{2} (\omega_c - \omega_r)^2 r_r^{\,4} \right) \tag{9}$$

The negative sign in Equation (9) indicates that the power is a loss, not a gain. Similar to the torque acting on the cylinder endface, Equation (9) shows that the power loss also has two components, namely the eccentric and the velocity difference components.

One example of this power loss profile is illustrated by Figure 4. The data is obtained based on the RV machine described in setion 2.2. The average total endface friction power loss of this machine is found to be 2.62 W. In

practice, it is important to remember that this power loss is for one side of the endface only. However, since a RV machine has two endfaces, the power loss should be doubled.
Figure 4 also shows that the eccentricity component is more dominant than the velocity difference one in this model. However, this may change for different RV machine designs.

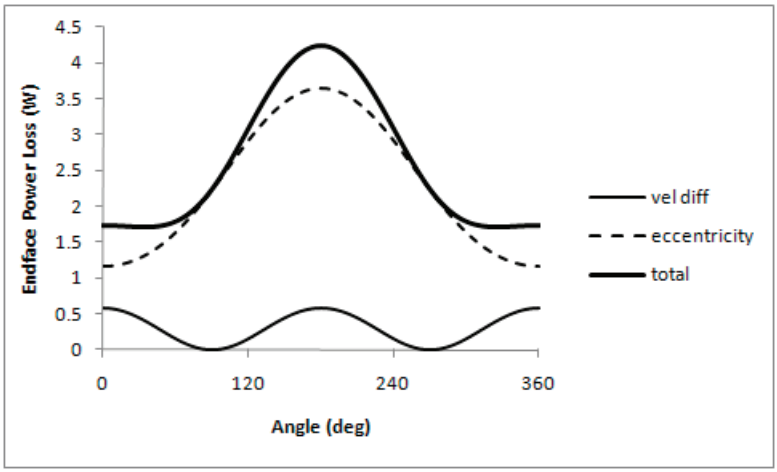

Figure 4: Endface power loss of a RV machine

The average power loss due to endface friction is obtained by taking the average of Equation (9) for one complete operating cycle, expressed by Equation (10).

$$\overline{P} = \frac{1}{2}\frac{\mu}{\delta} r_r^{\,2}\left(\pi r_r^{\,2}\omega_r^{\,2} - \left(e^2 + \frac{1}{2}r_r^{\,2}\right)\int_0^{2\pi}\omega_c^{\,2}\,d\varphi_r\right) \tag{10}$$

The second term of Equation (10) which contains an integral term is difficult to solve analytically. The angular velocity, ω_c, itself is expressed by Equation (11) and plotted in Figure 5 (Subiantoro and Ooi, 2009). Numerical integration may be performed to solve this integral term. Another method is to approximate the term with a simpler one. The second method is chosen here because by observing the cylinder angular velocity profile of the RV machine, the cylinder angular velocity seems to be able to be approximated with a cosine function expressed in Equation (12).

$$\omega_c = \omega_r\left(\frac{2(r_r + l_v)^2}{r_c^{\,2} + (r_r + l_v)^2 - e^2}\right) \tag{11}$$

$$\omega_c \approx \omega_r - (\omega_r - \omega_{c0})\cos\varphi_r \tag{12}$$

where ω_{c0} is the cylinder angular velocity when the operating angle is zero.

Comparing the averages of the cylinder velocities of the RV machine obtained from Equations (11) and (12) shown in Figure 5 shows that they agree very well. The root mean square difference is found to be only around 0.3%. This indicates that Equation (12) approximates Equation (11) very well. Using the approximated cylinder velocity in Equation (12), the average power loss per cycle can now be solved analytically and is expressed by Equation (13).

$$\overline{P} = -\frac{\pi}{2}\frac{\mu}{\delta}\left(\frac{r_r}{r_c}\right)^2 e^2\omega_r^{\,2}\left(3r_c^{\,2} - 2r_c r_r + 1.5r_r^{\,2}\right) \tag{13}$$

Using Equation (13), the average power loss of the RV machine presented in Section 2.2 is found to be 2.61 W which differs by only 0.3% from the real model.

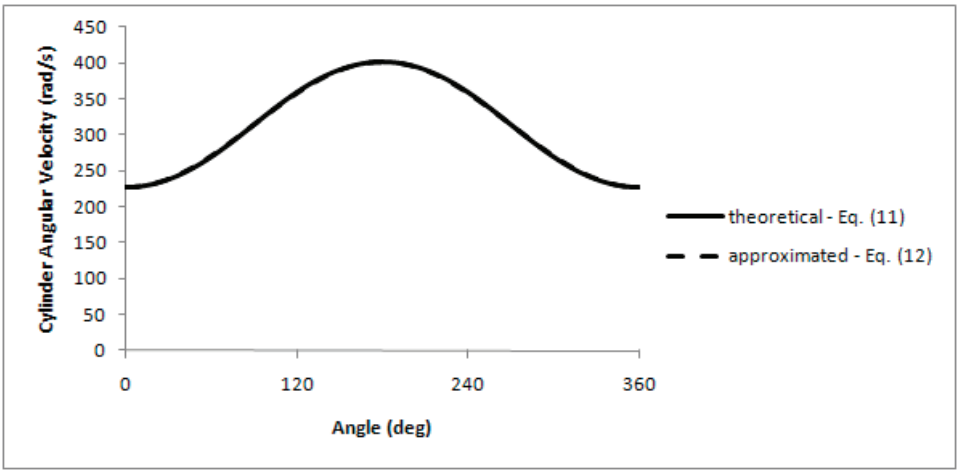

Figure 5: RV mechanism cylinder angular velocity

3. COMPARISON WITH STATIONARY CYLINDER MECHANISM

Most of the commonly found rotary machines have stationary cylinders. Therefore, it is intuitive to compare the RV mechanism results with those of the stationary cylinder ones. The area of interest is still assumed to be a solid circle as shown by Figure 2(b). The endface friction power loss can then be expressed by Equation (14).

$$P_0 = -\frac{\mu}{\delta}\frac{\pi}{2}\omega_r^{\,2} r_r^{\,4} \tag{14}$$

Unlike the RV mechanism power loss, Equation (14) has only the velocity difference component and does not have the eccentricity component. Of course the velocity difference is simply equal to the rotor velocity since the cylinder is stationary. In addition, since the rotor angular velocity is assumed to be constant, the instantaneous power loss is also the average power loss. Therefore, Equation (14) is also the average power loss expression.
It is also understood that the endface friction of the stationary cylinder mechanisms does not produce any resultant force since the relative velocity is purely rotational in nature, unlike the RV mechanism.

In order to compare the average power loss between the RV mechanism with that of the stationary cylinder, Equations (13) and (14) should be compared, producing a "loss ratio" expressed by Equation (15).

$$\frac{\overline{P}}{P_0} = 3\left(\frac{r_c}{r_r}\right)^2 - 8\left(\frac{r_c}{r_r}\right) + \frac{17}{2} - 5\left(\frac{r_r}{r_c}\right) + \frac{3}{2}\left(\frac{r_r}{r_c}\right)^2 \tag{15}$$

For the RV machine described in section 2.2, Equation (15) gives a value of 0.36, indicating that the RV endface power loss is significantly lower as compared to that of the stationary cylinder. Plotting Equation (15) against the "radius ratio" defined as the ratio between of the rotor and the cylinder radii (see Figure 6) shows that a RV mechanism produces lower endface loss than a stationary cylinder mechanism only if the radius ratio is larger than 0.6. Below this value, RV mechanism produces more endface loss than those of the stationary cylinder.

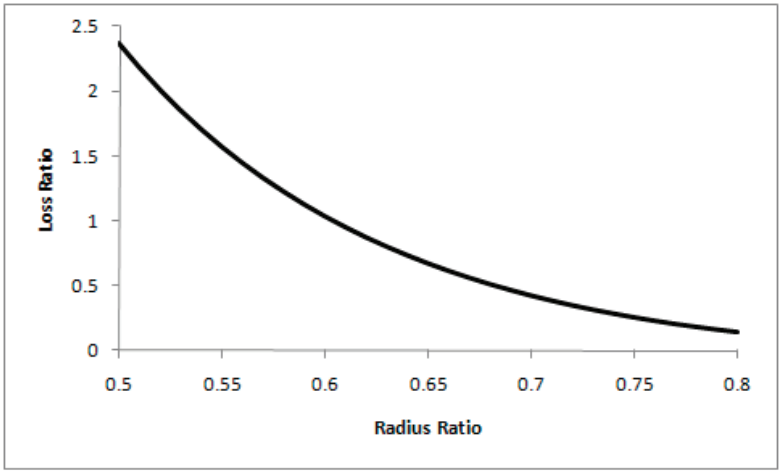

Figure 6: The loss ratio ($\overline{P} / P_0$) vs the radius ratio (r_r/r_c)

4. CONCLUSIONS

A theoretical study on the friction behavior in the RV mechanism endface gaps has been conducted. It is found that unlike in the cases of the common rotary machines, a resultant force is produced by the endface friction in RV mechanisms. This force is caused by the eccentricity of the mechanism and is proportional to the area of the rotor endface and the tangential velocity of the cylinder at the rotor axis. The analysis also shows that there is a region in between the rotor axis and the cylinder axis that suffers from high friction loss due to severe velocity difference occurring there.

The analysis on the power loss found that the RV mechanism endface friction power loss is not only affected by the velocity difference like those found in common rotary machines, but also by the eccentricity. Comparisons with common rotary machines show that RV mechanisms produce lower endface friction loss only if the ratio between the rotor and the cylinder radii is higher than 0.6.

NOMENCLATURE

A	area	(m^2)
e	eccentricity	(m)
F	force	(N)
l	length	(W)
P	power	(W)
r	radius	(m)
T	torque	(N.m)
V	velocity	(m/s)
x	variable distance	(m)
δ	endface gap	(m)
φ	angle	(radian)
μ	dynamic viscosity	(Pa.s)
τ	shear stress	(N/m^2)
ω	angular velocity	(rad/s)

Subscripts

0	stationary cyl.
c	cylinder
r	rotor
v	vane

REFERENCES

Subiantoro, A., Ooi, K.T., 2009, Introduction of the Revolving Vane Expander. *HVAC&R Res.*, vol. 15, no. 4: p. 801-816.

Subiantoro, A., Ooi, K.T., 2010, Design Analysis of the Novel Revolving Vane Expander in a Transcritical Carbon Dioxide Refrigeration System, *Int. J. Refrig.*, doi: 10.1016/j.ijrefrig.2009.12.023.

Teh, Y.L., Ooi, K.T., 2006, Design and Friction Analysis of the Revolving Vane Compressor, *Proc. Purdue Compr. Conf.*, no. C046: p. 1-7.

Teh, Y.L., Ooi, K.T., 2009a, Theoretical Study of a Novel Refrigeration Compressor - Part I: Design of the Revolving Vane (RV) Compressor and Its Frictional Losses, *Int. J. Refrig*., vol. 32, no. 5: p. 1092-1102.

Teh, Y.L., Ooi, K.T., 2009b, Experimental Study of the Revolving Vane (RV) Compressor, *Appl. Therm. Eng.*, vol. 29, no. 14-15: p. 3235-3245.

Yanagisawa, T., Shimizu T., 1985, Friction Losses in Rolling Piston Type Rotary Compressor. III, *Int. J. Refrig*., vol. 8, no. 3: p. 159-165.